Spring 5-2017

The Design and Fabrication of an Atomic Layer Deposition Reactor for Coating Powders

Natalie Altvater
University of Maine

THE DESIGN AND FABRICATION OF AN ATOMIC LAYER DEPOSITION REACTOR FOR COATING POWDERS

by

Natalie R. Altvater

A Thesis Submitted in Partial Fulfilment
of the Requirements for a Degree with Honors
(Chemical Engineering)

The Honors College

University of Maine

May 2017

Advisor Committee:

William DeSisto, Professor of Chemical Engineering
Melissa Ladenheim, Associate Dean of the Honors College
Michael Mason, Professor of Chemical and Biological Engineering
Thomas Schwartz, Assistant Professor of Chemical Engineering
Clayton Wheeler, Professor of Chemical Engineering

Abstract

Atomic layer deposition (ALD) is a self-limiting synthesis technique for the growth of conformal ultrathin films on solid state materials. The high conformality of the ALD method is ideal for coating porous, high surface area materials. A fluidized bed reactor (FBR) was designed and built for functionalizing a powder using ALD. The particle bed was fluidized using an inert argon gas. Aluminum oxide (Al_2O_3) was deposited on a high surface area powder substrate, γ-phase aluminum oxide, via ALD using trimethylaluminum (TMA) and water (H_2O) as gas phase precursors. Depositions were done under low pressure conditions. A BET analysis was done on the powder to confirm deposition of Al_2O_3 on the powder. Less coating was observed on the particles in comparison to literature.

Acknowledgments

I would like to thank my advisor Professor William DeSisto for his help, advice, and unfailing support throughout this project which would not have been possible without his support. I am also grateful to the professors of my committee, Melissa Ladenheim, Michael Mason, Thomas Schwartz, and Clayton Wheeler for their support and cooperation throughout this project. A special thank you to Nick Hill for his expertise in the lab. Finally, I want to thank my parents and friends for their unending encouragement outside of academics.

TABLE OF CONTENTS

List of Figures

List of Table

INTRODUCTION

Applications for nanoparticles in industrial and scientific areas have grown in the past couple decades. These particles are required to have a variety of bulk and surface properties to be used for said applications. The modification of powders to have functionalized surfaces can be accomplished by coating the individual particles with a nanometer-thick layer of a desired material. Several methods exist to accomplish this modification, but they were developed for use with planar substrates. Liquid-phase (sol-gel) and some gas phase (CVD) deposition techniques do not provide the conformal and ultrathin layer control necessary for making reproducible, scalable batches of powder.[1, 2] Atomic layer deposition (ALD) is a known method for depositing monolayers of conformal coatings. A variety of reactor configurations have been developed for coating a powder with ALD,[1] but this paper will focus on the use of a fluidized bed reactor (FBR).

The objective of this thesis is to develop a working fluidized bed reactor for coating a powder using atomic layer deposition. The use of gas-phase reactants in a FBR for the modification of a powder surface is not a new technique, and it can be scaled for use in industry to reliably create large batches of powder with high reproducibility. To demonstrate the effectiveness of the ALD reactor, the material used as a powder substrate is γ-alumina which can be used as a support for a metal catalyst, but it is considered on its own for this paper. The γ-alumina was coated with a Al_2O_3 film via ALD which has applications in improving a metal supported catalyst's life, selectivity, and activity.[3] γ-

Alumina is a porous material with a high surface area, so coating with sufficient monolayers will reduce the surface area. By monitoring the change in surface area, the success of the Al_2O_3 deposition reaction can be determined.

BACKGROUND

Atomic Layer Deposition

Atomic layer deposition (ALD) is a thin film synthesis method that allows for the continuous growth of monolayers on a solid surface. This technique is a subset of chemical vapor deposition, and involves sequential self-limiting reactions between alternating gas phase precursors and the solid surface. ALD takes place in a series of two half reactions where each vapor precursor chemisorbs to form a sub-monolayer on the surface. The reactions are self-limiting because after all the available reaction sites are used by the precursor the reaction ends. This characteristic ensures that every (sub)monolayer is deposited at the same thickness.

The first precursor is typically a high vapor pressure metal-organic such as trimethylaluminum (TMA). It is introduced to the solid surface and adsorbs to the surface by reacting with a certain functional group, such as a hydroxyl group. The precursor will adsorb on all exposed reaction sites including sites in holes, pores, trenches, etc. on the sample. Next, the precursor pulse is stopped before the unreacted precursor and any byproducts are removed from the reaction chamber either by evacuating at high vacuum or purging with an inert carrier gas, such as nitrogen or argon gas. Then the second precursor, usually an oxidant, saturates the reaction chamber and reacts with the metal-organic sub-monolayer to restore the reactive site present in the initial surface in preparation for the first precursor half reaction to begin again. Again, the pulse is

terminated after the second reaction reaches completion and the reaction chamber is purged. Figure 1 shows the steps of forming a monolayer as described above. The two half reactions displayed in Figure 1 are written here.

$AlOH_{(s)} + Al(CH_3)_{3(v)} \rightarrow AlOAl(CH_3)_{2(s)} + CH_{4(v)}$

$AlCH_{3(s)} + H_2O_{(v)} \rightarrow AlOH_{(s)} + CH_{4(v)}$

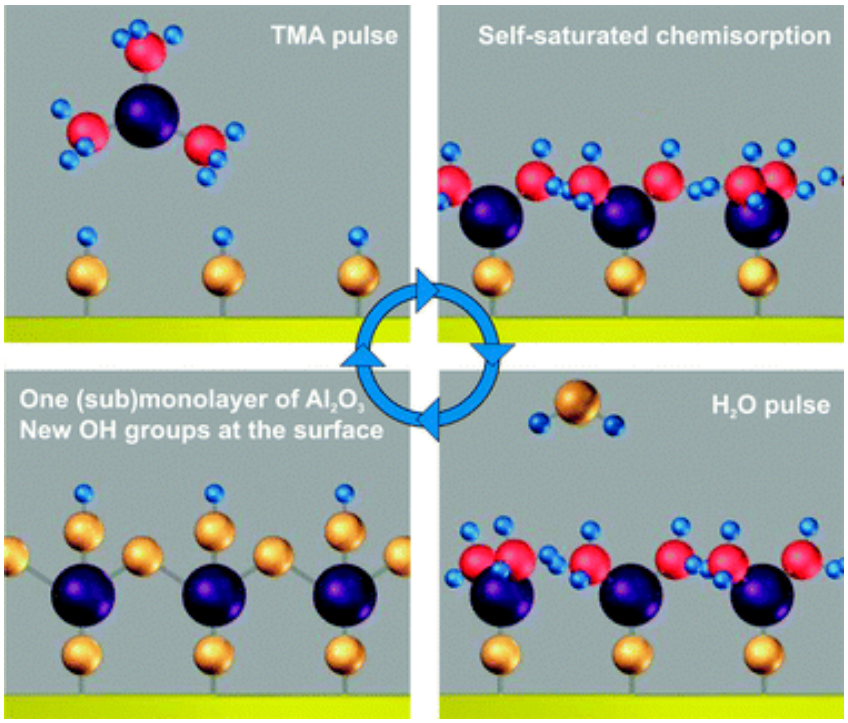

Figure 1. Diagram showing the deposition via ALD of one monolayer of alumina. Pulses of TMA and H_2O chemisorb onto the surface sites between inert gas purges.[4]

This A-purge-B-purge sequence creates one monolayer and allows for the precise control of film thickness. The AB binary precursor systems are typically driven by thermodynamically favored surface reactions. Other sequences involving three or more precursors in addition to the purge gas are also used. Methods such as ABC, ABCB, and A/C-B/C are used to make mixed oxides or carry out a catalyzed half reaction by introducing two precursors at once.

ALD offers several advantages over other deposition techniques such as chemical vapor deposition (CVD) and physical vapor deposition (PVD). CVD and PVD are both continuous methods not based on stepwise growth. Their growth rates are variable because they are determined by the rate and time of precursor exposure. Additionally, nucleation, which results in film discontinuities, is common with CVD and PVD. One advantage of ALD is that it can be performed with a wide array of materials used for precursors and substrates. Oxides, nitrides, sulfides, metals are the more common materials that have been deposited on solid state materials.[1, 2, 3, 4, 5, 6] Precursors must be stable, evaporable so that they can be deposited in vapor form, and must be able to react with the chosen substrate. Synthesis of organic and hybrid inorganic materials via ALD is a rising field for the modification of surfactants, polymers, and nanofibers.[4, 7, 8] Since ALD is not a line of sight process, materials with varying composition, porosity, roughness, and high aspect ratio can be uniformly coated. The self-limiting nature of the half reactions deposits that same amount of materials every cycle allowing for precise control of film thickness. By setting the number of precursor pulses ultrathin films (<10 nm) with Angstrom level precision can be made. This process is also chemically selective because adsorption to a surface is based on a chemical reaction at the surface. Depending on where these reactive sites are located on the substrate surface, this technique can be area selective. The surface reactions can be carried out at very low temperatures which is useful when working with temperature sensitive materials. ALD occurs through chemisorption, so the molecular self-assembly of layer formation reduces nucleation. As a result, the film has fewer discontinuities in the growth grain that would cause increased compressive stress in the final product. A major disadvantage to ALD is how slowly

films are made because each layer is only the thickness of the molecule deposited. However, this process can still be scaled for industrial applications because it is based on the surface area exposed to the precursor. Batch reactors can be designed to coat multiple materials at once.

ALD is currently used in several industrial applications for the modification of various materials. This technique is used in the microelectronics field for the modification and development of semiconductors.[4, 8, 9] Photovoltaic technology and other energy applications, such as fuel cells and batteries, utilize ALD as well.[4, 8] As mentioned previously, organic materials, including polymers, are also functionalized via deposition of both organic and inorganic precursors. Catalysis is another area where this technique is being used to fine tune the synthesis of catalytic materials.[3, 10] Additionally, previous processes that used CVD and PVD have increasingly turned to using ALD because of the advantages outlined above.[11]

ALD on Powders

ALD is an atomic level process and has many applications in the field of nanomaterials due to the conformity and precision film thickness control. Nanoparticles have many industrial and scientific applications, specifically in the pharmacy, petroleum, and chemical industries. Powders with functionalized surfaces are prepared and modified using a variety of methods (3). Methods using sol-gel techniques do not have the precision thickness control and conformity required for reproducible results when coating particles.[1, 2, 11] These liquid phase techniques involve multiple drying and separation steps before the powder can be modified. Even common gas-phase techniques, including CVD

and PVD, lack the film thickness control and conformity when dealing with porous particles. Industrial processes utilizing CVD often coat substrates with thicker layers than necessary to compensate for the inconsistent film growth. Clusters of particles, known as agglomerates, that form due to London-van Der Waals forces[12] in a bed of particles, can be coated as a whole when using CVD and sol-gel methods.[1] Coating the entire agglomerate instead of the individual particles is not favorable because permanent agglomerates form.[1] In contrast to these methods, ALD is not a line of sight process as discussed previously; therefore, it can evenly deposit materials with precise layer control without wasting unnecessary materials.

ALD Reactors for Coating Powders

Several types of reactors are used to coat powders using ALD. In the early 1990s ALD was performed on a static bed of particles with the precursor flowing down from above the substrate and diffusing down through it.[13] A similar design, but with the powder pressed into a tungsten grid support, was used in the early 2000s by Ferguson et al.[14] Another static particle ALD reactor uses a metal crucible to hold the powder while precursors are pumped across the particles.[1] These two reactor types demonstrate uniform deposition on various material, but they cannot be easily scaled to coat large amounts of powders for use on an industrial level. Fluidized bed reactors (FBRs), which will be the focus for the remainder of this report, have been shown to uniformly coat particles in scalable quantities.[1, 11] An FBR flows a carrier gas upward through a bed of particles supported on a frit.

A rotary reactor for agitated particles is another ALD deposition technique for coating powders without the long precursor times often required by FBRs.[1] This reactor uses a series of precursor pulses to agitate the particle bed and raise reactant efficiency by increasing contact time between the static precursor and substrate.

Fluidized Bed Reactor for ALD

Fluidized bed reactors offer several advantages over the designs mentioned above when considered for application on an industrial scale. First, the nature of a FBR makes it scalable and therefore, useful for industrial production where large quantities of powders need to be made with consistency. In contrast to planar substrates, powders present with an exponentially larger surface areas as well as pores that the precursor must diffuse through necessitating longer pulse times for the reaction to complete at all the surface sites. Gas-solid fluidization allows for a large contact efficiency because of the physical mixing and agitation that comes from fluidization. This mixing is important to ensuring all surface reaction sites are brought into contact with the precursor. FBRs offer a degree of physical mixing that is not found in rotary or static bed reactors. Reactors using grids or crucibles to support the substrate have limited precursor gas transport. Particles at the surface of the bed will be sufficiently coated, but at depths of more than a few microns the gas will not diffuse to the bulk of the particle bed leaving it uncoated. Fluidization eliminated this issue. The high surface area of powders also means that the surface area of the reactor walls is relatively small. As a result, less precursor will be lost to the walls, and it will be more efficiently used because the gas passes through the bed with a high contact efficiency as mentioned above.

For a bed of particles to be fluidized, a gas must be pushed upward through the bed of particles at a specific velocity. As the velocity of the gas entering the reactor increases, the upward drag force of the gas matches the downward force of the particle due to gravity. At this minimum fluidization velocity, the particles will lift from the bed which fractionally increases the distance between all particles expanding the bed. If the velocity continues to increase, particles will become further separated as the particle motion becomes more volatile until the particles flow with the gas. A pressure drop occurring across the reactor is caused by the resistance to flow from frictional forces and the particles' weight. A higher gas velocity means a larger pressure drop until the minimum fluidization velocity is reached. At this point the pressure drop will remain constant even if the fluidizing gas velocity increases further.

Another advantage of FBRs for ALD is that they function over a large range of pressures. Because fluidization is dependent on the pressure drop across the bed, FBRs can operate from ambient to vacuum pressures. Low operating pressures are preferable for ALD to aid in the vapor phase adsorption of precursors onto the solid substrate. The minimum fluidization velocity is another important characteristic of a FBR. This velocity is influenced by particle size, particle density, and gas properties. Calculations for minimum fluidization velocity were done based on the work of Llop et. al.[15] for fluidization at vacuum conditions, and will be discussed later in the report. Under vacuum/near vacuum conditions a state of bubbling fluidization is achieved. Bubbling fluidization differs from the homogeneous fluidized bed described above in which particle separation increases linearly with increasing gas velocity while the pressure drop remains constant (after minimum fluidization velocity is reached). In a bubbling fluidized

bed (described in depth by Tommey and Johnstone[16]), the particle bed expands under fluidization and any excess gas beyond what is needed for fluidization escapes in the form of bubbles. For small, light particles, the minimum gas velocity where bubbling appears is greater than the minimum fluidization velocity. Thus, the appearance of bubbles indicated that the particle bed is fluidized.

Fluidization Calculations

Minimum fluidization velocity (u_{mf}) was calculated for fluidization at vacuum conditions using calculations derived by Llop et. al.[15] For this calculation the gas properties of argon gas as well as the particle characteristics were the primary influences. Because the batches of sieved particle were made with a range of sizes, an average of the largest and smallest diameters was used in calculations. The shape factor for this powder was assumed to be round ($\varphi > 0.8$) which is a reasonable assumption for the purposes of this paper. Minimum fluidization velocity can be found using Reynolds number, Equation 1.

$$u_{mf} = \frac{Re_{mf}\mu}{\rho d} \tag{1}$$

Here, μ is the gas viscosity, ρ is the gas density, and d is the reactor diameter. An expression for Reynolds number at minimum fluidization (Re_{mf}) for round particles was derived by Llop and is shown in Equation 2. Several simplifying assumptions on the shape factor of round particles and its relation to the reactor bed voidage at incipient fluidization were made to develop Equation 2.[15]

$$Re_{mf} = \sqrt{\left(\frac{0.909}{Kn_p+0.0309}\right)^2 + 0.0357Ar} - \left(\frac{0.909}{Kn_p+0.0309}\right) \tag{2}$$

Archimedes number (Ar) and the Knudsen number of the particle (Kn_p), shown in Equations 3 and 4, must be determined for the Reynolds number equation.

$$Ar = \frac{\rho(\rho_s - \rho){d_p}^3 g}{\mu^2} \tag{3}$$

Here the substrate density is ρ_s, d_p is the particle diameter, and g is acceleration due to gravity. Archimedes number is a dimensionless value used to represent the ratio of buoyancy and internal forces to characterize the motion of fluids caused by differences in density.

$$Kn_p = \frac{\lambda}{d_p} \tag{4}$$

In Equation 4, for the Knudsen number, λ is the mean free path (Equation 5) of the argon gas particle. Kn_p is another dimensionless value that characterizes the flow regimes in which fluidized beds can exist.[15] Fluidization can occur when $Kn_p \approx 1$ or $Kn_p << 1$ which correspond to slip flow and laminar flow respectively. In this region, the continuum mechanics can be used for fluid dynamic calculations.[17]

$$\lambda = \frac{kT}{\sqrt{2}\pi p {d_g}^2} \tag{5}$$

In Equation 5, k is Boltzmann's constant, T is the operating temperature of the reactor, and p is the pressure inside the reactor. The mean free path of a gas molecule is the average distance traveled by moving particles between collisions with each other.

ALD of Alumina

The solid substrate used to demonstrate ALD on a bulk powder, was γ-alumina also known as aluminum oxide. γ-Alumina (γ-Al_2O_3) is a highly porous material that is used extensively as a catalyst and catalyst support in the petroleum industry. The highly

porous nature of this material results in a high surface area (210 m^2/g) which is a favorable characteristic for catalytic applications. The microstructure can be seen in Figure 2. γ-Alumina has a cubic crystal lattice with layers of cubic close packed oxygen atoms and aluminum atoms in the tetrahedral and octahedral sites.[18] Several of the lattice sites are unoccupied so that the stoichiometry of Al_2O_3 is consistent. The exact location of these empty lattice sites is disputed.[10] While this oxide can be used as a support for a metal catalyst, here it will be considered in its pure form.

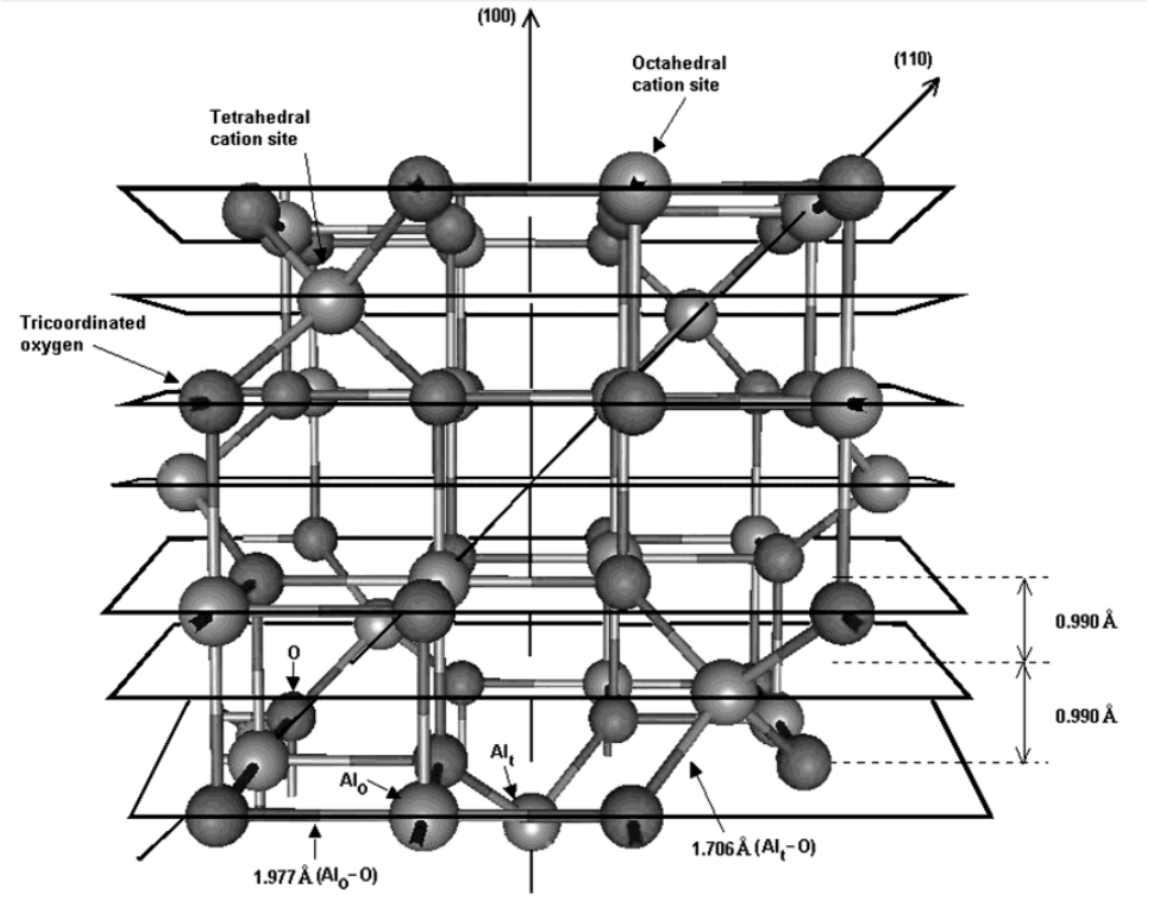

Figure 2. Crystal structure of γ-alumina unit cell showing cubic close packing of oxygen atoms with aluminum atoms at tetrahedral and octahedral sites.[19]

The thin film deposited by ALD was aluminum oxide (Al_2O_3), a coating that has been demonstrated in previous studies.[20] Deposition of an Al_2O_3 film is a model ALD

system because of the highly efficient and self-limiting nature of the reaction. The strong Al-O bond formed is the driving force behind the efficient reactions. This primary reaction is the basis for the coating process:

$$2Al(CH_3)_3 + 3H_2O \rightarrow Al_2O_3 + 6CH_4 \quad (1)$$

ALD takes place in two separate half reactions as discussed previously. Trimethylaluminum (TMA) and water (H_2O) were used for these reactions:

$$AlOH^* + Al(CH_3)_3 \rightarrow AlOAl(CH_3)_2^* + CH_4 \quad (2)$$

$$AlCH_3^* + H_2O \rightarrow AlOH^* + CH_4 \quad (3)$$

The * denotes the surface species. These precursors were exposed to the powder in an alternating ABAB reaction sequence. At temperatures over the range of 177°C to 300°C the amount of alumina adsorbed in the TMA reaction decreases because this is the temperature at which TMA begins to thermally decompose.[6, 8] Al_2O_3 film growth is highly linear with the number of cycles, and this layer growth has been characterized using methods like spectroscopic ellipsometry and quartz crystal microbalance measurements. One monolayer deposited in an AB cycle is approximately 1.1-1.2 Å thick.[8] Argon gas was used as the inert fluidizing gas as well as the purge gas between precursors.

ALD Precursor Exposure

For surface saturation to occur at the γ-alumina surface sites during each half-reaction, sufficient pulse times (precursor dosage) must be used. Typical exposure or dosage of a vapor to a solid surface is measured in Langmuir. A Langmuir (L) is the product of the gas vapor pressure and the and the exposure time,[21] where one Langmuir

corresponds to the exposure of a surface to 10^{-6} torr for one second. An ALD system for depositing alumina on a planar silicon surface used exposures of approximately 2×10^5L.[22] Ferguson[20] reported that an exposure of 10^8 L was necessary for complete surface coverage on BN particles with a surface of 300 m^2/g. Other authors[23] report that the surface functional group concentration[24] requires $10^6 – 10^8$ L for complete coating of alumina on BN particles. The target exposure used here was 10^8 L. Achieving the desired exposure can be accomplished by adjusting the reactant vapor pressure or the pulse time. Vapor pressures were set using the precursor temperatures. Equation 6 displays the calculation for minimum pulse times.

$$t_p = \frac{E}{vp} \tag{6}$$

Here t_p is exposure time, E is the target exposure, and vp is the vapor pressure. The pulse times were then increased by a factor of 10 to allow sufficient time for the vapor precursor to saturate the porous substrate. Equation 6 is designed for the coating of planar substrates, but powders require additional dosage time due to higher surface area and diffusion limitations in pores. Dosing times for a similar Al_2O_3 ALD system reported by Wiedmann et. al.[25] ranged from 30-600 s. To ensure complete precursor saturation in the first monolayer, exposure times were doubled[25] for deposition of the first layer.

Measurement of Surface Area Reduction by ALD

γ-Alumina has a surface area[10] of approximately 210 m^2/g due to the porous nature of the powder. O'Neill et. al. reported that 45 coats of alumina via ALD on a γ-alumina supported copper catalyst resulted in a 99.0% reduction in surface area.[10] This analysis was done using the Brunauer-Emmett-Teller (BET) analysis method. During

analysis, the volume of gas adsorbed to the sample surface is correlated to surface area of a solid. The BET theory for multilayer adsorption operates on several assumptions: (1) each molecule in a layer is an adsorption site for the next layer, (2) the rate of adsorption is the same for each layer, and (3) the heat of adsorption in the second layer (and those above it) equals the heat of liquefaction of the adsorbate.[26] Physical adsorption, or physisorption, is a process where gas molecules (adsorbate) adhere to a surface (adsorbent) due to attractive Van der Waals forces.[27] Physisorption is reversible because of the weak nature of the bonds, and it is a non-selective process meaning the entire surface will be layered with gas molecules (pores, holes, etc.). An adsorption and desorption curve plotted against pressures is called an adsorption isotherm (Figure 3). Because the desorption curve lags the adsorption, a hysteresis loop is apparent in the plot. Hysteresis loops happen because the rate of desorption is affected by the capillary condensation in pores. The vapor fills pores whose openings are smaller than the body, so desorption will occur at lower relative pressures and the pores empty suddenly instead of gradually, the way they were filled.[28]

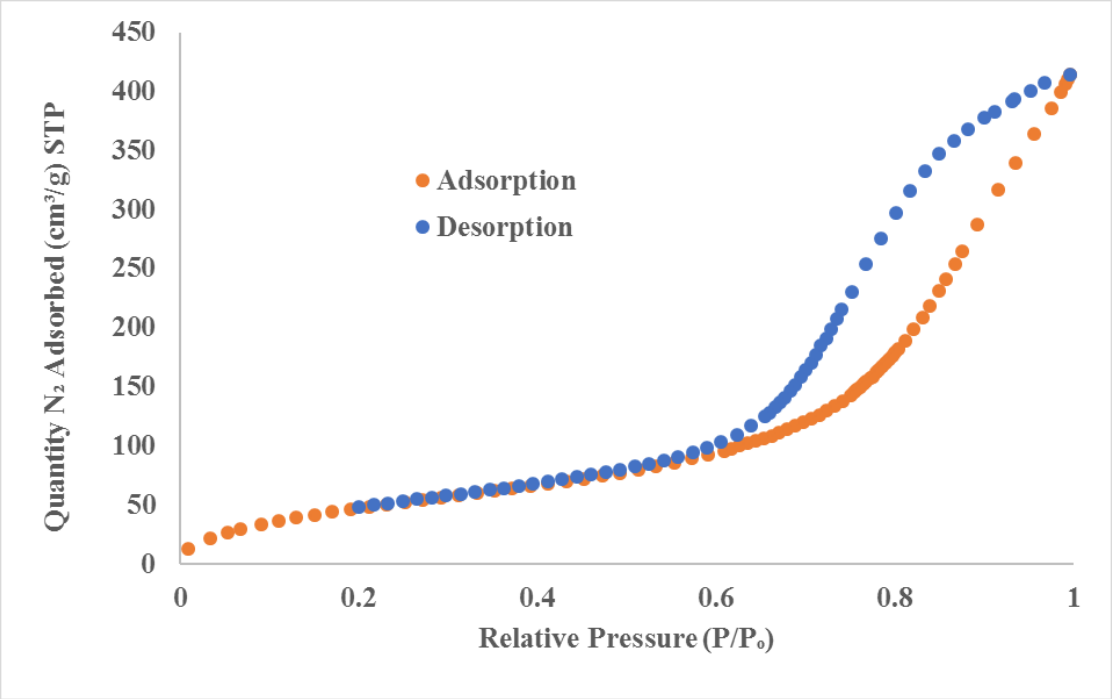

Figure 3. BET isotherm of nitrogen gas adsorption/desorption onto γ-alumina powder that has been coated with Al_2O_3 via ALD. Analysis done on the ASAP 2020 Plus Physisorption instrument (Micromeritics Instrument Corporation, GA).

To measure surface area, the amount of gas adsorbed on a saturated surface is correlated to the total surface area using isotherm data and the BET equation (Equation 7).

$$\frac{P}{V(P_o - P)} = \left[\frac{(C-1)}{V_m C}\right]\frac{P}{P_o} + \frac{1}{V_m C} \tag{7}$$

Here V is the total volume of gas adsorbed, P is the operating pressure, V_m is the volume adsorbed at monolayer coverage, P_o is the adsorbate vapor pressure, and C is the BET constant which is specific to each adsorbate.[26] After solving this equation for V_m, specific surface area (A) is calculated from Equation 8.[26]

$$A\left(\frac{m^2}{g}\right) = \frac{\left((V_m, \frac{cm^3 STP}{g}\right)\left(\frac{6.023\times10^{23}\ molecules}{21400 cm^3\ STP}\right)}{\left(\frac{cross\ sectional\ area, m^2}{molecule}\right)} \tag{8}$$

All BET calculations were done by the software within the BET instrument. To determine if the reactor was effectively depositing Al_2O_3 layers on the substrate, before and after BET measurements were taken to observe the change in specific surface area.

METHODS AND MATERIALS

γ-Phase aluminum oxide pellets (Alfa Aesar, MA) were ground and sieved to 90-180 micron or 180-425 micron. Trimethylaluminum was purchased from Sigma-Aldrich pre-loaded in a ALD bubbler. Deionized water was loaded into an ALD bubbler. Grade 5.0 argon gas (BOC) was used as the purge and fluidizing gas. This gas was passed through a Matheson gas purifier (model 450B) prior to use.

Reactor Configuration

The coatings done by ALD were carried out in a fluidized bed reactor build based on designs by King et. al. and Wank et. al.[11, 23] Two different reactors of with diameters of ¼" and 1" were built and tested. The substrate was ground and sieved in batches of 2-5 g at a time to 180-90 micron and 425-180 micron for use in the ¼" diameter and 1" diameter reactors respectively. The ¼" reactor was plexiglass with a stainless-steel screen 250 mesh (58 micron) that acted as a frit to support the powder. The 1" reactor was made of Pyrex glass tubing with a P0 glass frit (pore size 160-250 micron). Both reactors were made to allow visual inspection of the fluidization process.

The outlet of the reactor was attached to a rotary vane vacuum pump (Marathon Electric, WI) as shown in Figure 4. The roughing pump allowed the pressure in the reactor to be reduced to 27 millitorr. During fluidization pressures ranged from 90 to 500 millitorr. A pressure gauge was located at the line between the reactor outlet and pump. A hand-operated, shut-off valve located prior to the pump was used to gradually expose the particle bed to vacuum. Inert argon gas, regulated by a mass flow controller (MKS

Instruments Inc.) was fed to the reactor as a purge gas to maintain fluidization during purge and dosing stages. The precursors of deionized water and TMA were held in bubblers that had one outlet leading to a gas chromatographic (GC) valve. This valve had four ports that allowed either argon gas, TMA, or H_2O to be isolated to a set inlet with one common outlet. One port not in use was sealed to avoid leakage in the system. The argon gas (1) port on the valve was not used as a purge gas. Instead a separate argon gas line, joined after the rotating valve just prior to the reactor inlet was used to fluidize the particle bed. The GC valve setting was controlled manually. The GC valve allowed for rapid switching between the precursors which is essential during fluidization. If the switch between gasses is not done rapidly the gas velocity will drop causing the particle bed to collapse. If this occurs the reactor will experience interrupted mixing which reduces the exposed particle surface area due to poor mass transfer.

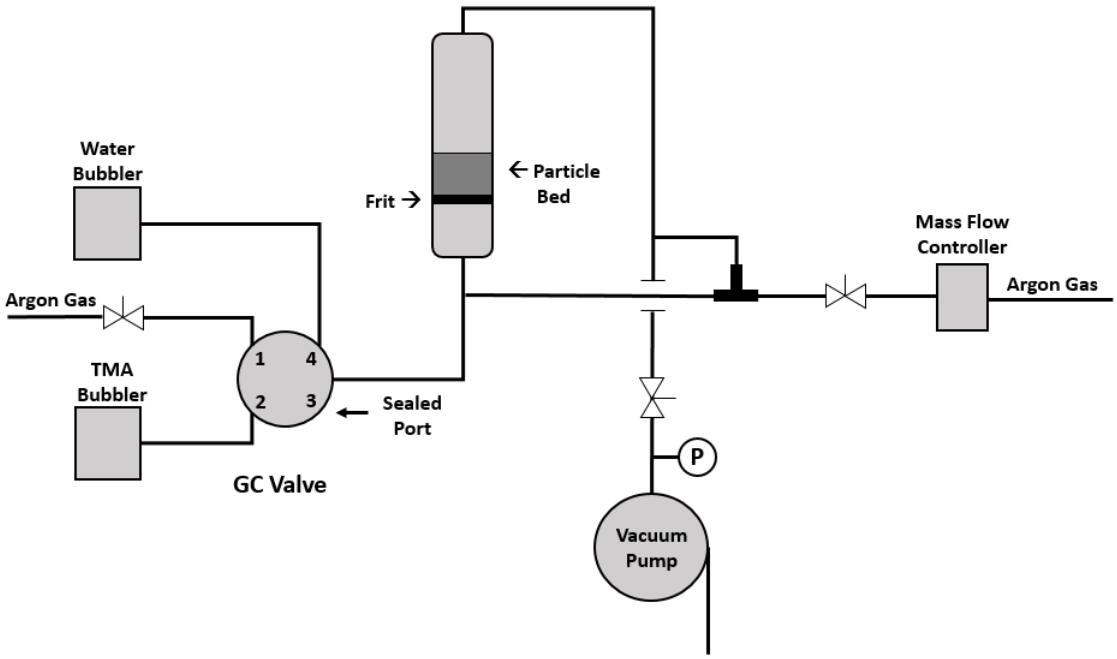

Figure 4. Schematic of the fluidized bed reactor setup used for ALD of Al_2O_3

To avoid a large pressure drop across the reactor when opening the pneumatic valve to the argon gas for fluidizing, a three-way valve was installed to connect the primary argon gas line to the reactor outlet line as seen in Figure 4. By initially diverting the argon gas to the pump, the reactor is opened to the gas stream so that the near vacuum pressure in the reactor can equalize. If the pneumatic valve was opened directly to the particle bed, which was at low pressure conditions, the powder would flush to the top of the reactor. Even with the mass flow controller at the lowest possible setting (2 sccm) the violent bed agitation on initial exposure lodged particles in the upper screen of the ¼" reactor. This effect was more pronounced with the smaller diameter reactor, but could be avoided entirely in the 1" reactor with the modification described above.

The reactor and lines reaching from the bubbler outlets to the reactor inlet were wrapped in heat tape and connected to a variable autotransformer (Staco Energy Products, OH). The lines were maintained at 115°C while the reactor was held at 120°C. The rotating valve was also heated to 115°C. Elevated temperatures prevent condensation of the precursor vapor in the lines, and the γ-alumina ALD reaction rates increase with higher temperatures. A chiller (Isotemp 2150 Nano Circulator, Fisher Scientific) was attached to both bubblers keeping the precursors at 20°C. At this temperature, the vapor pressure of H_2O is 17.5 torr and TMA is approximately 9 torr. Higher temperatures for the precursors mean a higher vapor pressure. At higher vapor pressures, shorter pulse times are needed to saturate the reactor for complete reaction at the particle surface sites.

A single reaction cycle for deposition of one monolayer was TMA-purge-H_2O-purge. Pulse times used for TMA and H_2O were 180 s and 120 s respectively which correspond to $1.6x10^9$ and $2.1x10^9$ L. Precursor pulse times were doubled for the first

cycle. Argon gas purge times were held constant at 8 min which fell in the 6-10 min range for purge times reported in similar systems.[10, 25] The flow rates determined for the argon fluidization gas were 0.56 sccm and 3.95 sccm for the ¼" and 1" reactors respectively.

BET Surface Area Measurement

The ASAP 2020 Plus Physisorption instrument (Micromeritics Instrument Corporation, GA) was used for all BET measurements. In preparation for analysis, the powder sample (approximately 0.1g) was placed under high vacuum while being heated at 100°C to degas and dry for 12-16 hrs. The analysis was done using nitrogen gas for the physisorption while the sample was held in a liquid nitrogen bath. The ASAP 2020 produced specific surface area (m^2/g) measurements on the powder samples before and after ALD coating using the BET isotherms described previously.

RESULTS

To visually confirm fluidization of the powder bed, both reactors were operated at room temperature without the heat tape so that particle behavior could be observed. The reactor is shown in Figure 5 with a fluidized particle bed. The minimum fluidization velocity calculated for the ¼" reactor was 24 cm/s. At this velocity, 0.56 sccm of argon gas were required for fluidization. The lowest setting on the mass flow controller was 1.5 sccm so the smaller reactor could not be operated at the minimum velocity. The transition from a static bed to an expanded, fluidized bed at u_{mf} could not be observed. Instead the particle bed immediately expanded beyond the point of bubbling fluidization and experienced violent agitation causing some of the powder to become lodged in the screen at the top of the reactor. Even after installing a three-way valve to divert the initial flow of argon gas, as described previously, the u_{mf} could not be observed in the ¼" reactor.

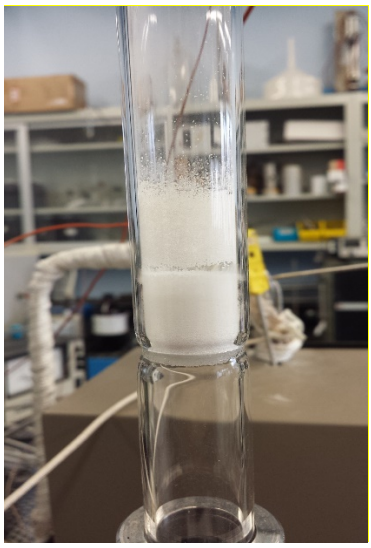

Figure 5: Image of the reactor without the heat tape so that the particle bed fluidization could be visualized.

In the 1" diameter reactor u_{mf} was 70.5 cm/s which translated to 3.95 sccm. In this configuration, the transition from a static to fluidized bed could be observed. A marginally expanded particle bed was observed at an argon gas flow rate of 4 sccm. Bubbling fluidization was observed at 4-5 sccm which corresponds to 71.5-89.4 cm/s. Bubbling fluidization happens when a low-pressure system passes minimum fluidization. The reactor was operated at bubbling fluidization to ensure that the bed was properly fluidized.

Due to the difficulty in operating the ¼" diameter reactor at minimum conditions, only one of the samples from a coating trial done with this reactor was analyzed. Most trials were run on the larger 1" diameter reactor. The specific surface area measured for the uncoated γ-Al_2O_3 was 230 m^2/g. This value is comparable to the value of 210 m^2/g reported elsewhere.[10]

Table 1. Experiment Table for ALD trials to compare operating conditions to surface area reduction.

Trial	Reactor Diameter (in)	Powder Load (g)	Precursor Temp. (°C)	Purge Time (s)	TMA Dose (s)	H_2O Dose (s)	No. cycles	Coated S.A. (m^2/g)	Reduced S.A. (%)
1	1/4	1.00	10	240	180	120	10	225.43	1.99
2	1	2.01	10	240	180	120	30	222.75	3.15
3	1	2.00	10	240	180	120	30	228.45	0.674
4	1	0.53	20	480	180	120	20	191.78	16.6

Table 1 contains the results of the primary trials done with the reactor. During trials pulse and purge times were timed and changed manually. If a trial could not be completed at one time, the system was left under vacuum at the end of a cycle and remaining cycles were completed later.

The coated powder in the ¼” reactor did not exhibit the estimated drop in surface area. Due to the startup issues with this size reactor, few trials and no duplicates were run in the ¼” reactor. The 1” diameter reactor was able to hold more powder, but the expected change in surface area was not observed. Trial 3 is a duplicate of trial 2, and both had a negligible change in surface area. Trial 4 had the most coverage.

DISCUSSION

The effectiveness of the reactor in depositing Al_2O_3 via ALD on the powder substrate was quantified based on the change in total surface area of the γ-alumina. In a similar system[10] forty-five coatings of alumina reduced the surface area by 99%. Coverage increases linearly with the number of ALD coatings. Although this reactor was different than the system built here, these values were used to estimate surface area decrease from the number of layers. Bases on the ratio of layers to surface area reduction, twenty coatings would result in approximately a 44% reduction. As shown in Table 1, the values recorded did not match values found in the literature. The powder was coated less than expected. Trial 4, with the higher precursor temperatures and longer purge time, had the most coating. The 16.6% reduced surface area is still less than half the estimated 44%. There are several reasons why the results do not match the values reported in the literature.

First, an equipment issue was observed when dosing the H_2O precursor. The reactor pressure baseline was 90-100 millitorr during fluidization, without any precursor dosing. When the GC valve was opened to the TMA bubbler, the reactor pressure increased 350-400 millitorr above the baseline and remained for the duration of the exposure time. This expected increase in pressure was not observed when dosing the H_2O precursor. When the GC valve was opened to feed H_2O to the reactor, pressure increased 15-30 millitorr above the baseline then immediately fell back to baseline pressure. No increase in pressure from the H_2O vapor meant that the flow of precursor to the reactor was insufficient to saturate the particle bed. This suggests that the quantity of vapor

decreased during the exposure time resulting in an exposure much less than the exposure time set point. Even when the vapor pressure was increased, from 9.2-17.5 torr, by raising the bubbler temperature from 10-20 °C, the same pressure behavior as described above was observed. The lack of proper precursor exposure could explain the low ALD coating.

Another potential downfall of the system is that mechanical agitation was not used to prevent particle agglomeration. The use of a vibro-motor or a mechanical stirrer was not incorporated to aid fluidization for this design due to size constraints. A vibro-motor would aid in fluidization and prevent the formation of agglomerates via mechanical agitation. Agglomerates form during fluidization when the particles temporarily leave the bed zone in clusters. These aggregates are dynamic (soft), meaning that individual particles transfer in and out of aggregates. When the powder is properly fluidized, the rapid exchange of particles ensures that all particles are effectively coated by ALD.[11] There is a danger of an entire agglomerate being coated and fixed in that state, but proper fluidization should prevent this case. Bed segregation can occur under vibro-fluidization in the case of a large particle size distribution because this method causes pulsating in the axial direction. These mechanical additions can assist in fluidizing the bed and eliminating aggregates at lower gas velocities, but their benefits are more evident when dealing with larger scale (50 g bed) operations than what was considered for this project.[11] If the particles were coated in agglomerates then the particles on the inside would not be sufficiently exposed to the precursors. As a result, a portion of the particles would remain uncoated or partially coated, leaving them with a high surface area.

If the bed was not always sufficiently fluidized during the coating process incomplete coating can result. Although bubbling fluidization in an expanded particle bed was observed, the pressure difference across the particle bed was not monitored to verify fluidization. Even in the case of adequate fluidization, the particle bed could experience incomplete mixing. If channeling occurred, meaning the gas flow is greater at some points than others, not all particles would be equally exposed to the precursors. Channeling would result in pockets of powder where the surface is not fully saturated during each precursor dose. Due to features like pores, holes, and trenches, surface reactions are transport-limited in particles, causing reaction at the pore entrance to happen first. Non-conformal films can result when CVD type deposition occurs at the opening of pores and trenches.[29] This non-self-limiting growth can be caused by a higher partial pressure of reactant at the top of a trench than the bottom. This deviation from the ideal ALD process would cause incomplete particle coating.

RECOMMENDATIONS & CONCLUSION

Path Forward

The extent to which each of the above-mentioned issues impacted the ALD process is unknown. However, several steps can be taken to resolve or reduce these problems. First, the H_2O line and bubbler should be inspected. A blockage or leak in the tubing surrounding the H_2O would prevent the precursor from reaching the reactor. Verifying that this precursor delivery line is in working order would be the first step before further experiments.

The exposure to precursors must be increased so that the surface sites can be fully saturated during each pulse. In Trial 4, the amount of powder in the reactor was decreased from 2g to 0.53g. Although other factors were changed in this trial, reducing the material in the reactor is recommended for future trials. Less material means a smaller surface area needs to be saturated. Mechanical agitation, in the form of a vibro-motor or a mechanical stirrer should be added to the reactor configuration. Mechanical agitation will not only reduce the formation of agglomerates, but it will also aid in fluidization. If the aggregates are broken up more rapidly, the inner particles will be exposed to the precursors and not only the outer particles will be coated.

To ensure that the powder bed is properly fluidized, a pressure sensor should be added before the reactor. This would allow monitoring of the pressure drop across the reactor to better determine the gas flow rate for fluidization.

The precursor pulse times used were longer than theoretically required. While the longer pulse times were used to ensure surface saturation, they also waste precursor. Adding a residual gas analyzer to the system configuration could monitor precursor concentration and determine when the surface is saturated. In the system used by Wiedmann as well as other authors[10, 11, 25], a residual gas analyzer was used at the outlet of the reactor to monitor the residual gas. With this configuration, the pulse times were terminated when the levels of byproduct gas dropped and the exit gas changed primarily the precursor vapor. This method allowed precise monitoring of the coating process so that the precursors were not wasted with unnecessarily long pulse times. Implementing a RGA would be useful to better monitor the film growth process and efficiently use the precursors.

In conclusion, a fluidized bed reactor for coating a powder by atomic layer deposition was designed and implemented. The γ-alumina powder was coated as evidenced by a reduction in surface area. Discrepancies with results reported in the literature for similar reactor systems will require further analysis and experimental planning.

REFERENCES

1. Longrie D, Deduytsche D, Detavernier C. Reactor concepts for atomic layer deposition on agitated particles: A review. Journal of Vacuum Science & Technology A: Vacuum, Surfaces, and Films. 2014;32(1):010802.

2. Detavernier C, Dendooven J, Pulinthanathu Sree S, Ludwig K, Martens J. Tailoring nanoporous materials by atomic layer deposition. Chemical Society Reviews. 2011;40(11):5242.

3. O'Neill B, Jackson D, Lee J, Canlas C, Stair P, Marshall C Et al. Catalyst Design with Atomic Layer Deposition. ACS Catalysis. 2015;5(3):1804-1825.

4. Ultratech. Atomic Layer Deposition - Ultratech/CNT [Internet]. Cambridgenanotechald.com. 2016 [cited 15 April 2017]. Available from: http://www.cambridgenanotechald.com/atomic-layer-deposition/index.shtml

5. Mastai Y. Materials science - advanced topics. 1st ed. Rijeka, Croatia: INTECH; 2014.

6. Puurunen R. Surface chemistry of atomic layer deposition: A case study for the trimethylaluminum/water process. Journal of Applied Physics. 2005;97(12):121301.

7. George S, Yoon B, Dameron A. Surface Chemistry for Molecular Layer Deposition of Organic and Hybrid Organic−Inorganic Polymers. Accounts of Chemical Research. 2009;42(4):498-508.

8. George S. Atomic Layer Deposition: An Overview. Chemical Reviews. 2010;110(1):111-131.

9. Wank J, George S, Weimer A. Vibro-fluidization of fine boron nitride powder at low pressure. Powder Technology. 2001;121(2-3):195-204.

10. O'Neill B, Jackson D, Crisci A, Farberow C, Shi F, Alba-Rubio A et. al. Stabilization of Copper Catalysts for Liquid-Phase Reactions by Atomic Layer Deposition. Angewandte Chemie International Edition. 2013;52(51):13808-13812.

11. King D, Spencer J, Liang X, Hakim L, Weimer A. Atomic layer deposition on particles using a fluidized bed reactor with in situ mass spectrometry. Surface and Coatings Technology. 2007;201(22-23):9163-9171.

12. Visser J. Van der Waals and other cohesive forces affecting powder fluidization. Powder Technology. 1989;58(1):1-10.

13. Lindblad M, Haukka S, Kytökivi A, Lakomaa E, Rautiainen A, Suntola T. Processing of catalysts by atomic layer epitaxy: modification of supports. Applied Surface Science. 1997;121-122(0169-4332):286-291.

14. Ferguson J, Weimer A, George S. Atomic layer deposition of Al2O3 and SiO2 on BN particles using sequential surface reactions. Applied Surface Science. 2000;162-163:280-292.

15. Llop M, Madrid F, Arnaldos J, Casal J. Fluidization at vacuum conditions. A generalized equation for the prediction of minimum fluidization velocity. Chemical Engineering Science. 1996;51(23):5149-5157.

16. Toomey R, Johnstone H. Gaseous Fluidization of Solid Particles. Chemical Engineering Progress. 1952;48(5):220-226.

17. Barber R, Emerson D. Advances in Fluid Mechanics IV. Edited by M. Rahman, R. Verhoeven & C. A. Brebbia. Journal of Fluid Mechanics. 2002;475:736-741.

18. Trueba M, Trasatti S. γ-Alumina as a Support for Catalysts: A Review of Fundamental Aspects. ChemInform. 2005;36(44).

19. Ionescu A, Allouche A, Aycard J, Rajzmann M, Hutschka F. Study of γ-Alumina Surface Reactivity: Adsorption of Water and Hydrogen Sulfide on Octahedral Aluminum Sites. The Journal of Physical Chemistry B. 2002;106(36):9359-9366.

20. Ferguson J, Weimer A, George S. Atomic layer deposition of ultrathin and conformal Al2O3 films on BN particles. Thin Solid Films. 2000;371(1-2):95-104.

21. Gordon R, Hausmann D, Kim E, Shepard J. A Kinetic Model for Step Coverage by Atomic Layer Deposition in Narrow Holes or Trenches. Chemical Vapor Deposition. 2003;9(2):73-78.

22. Yue Z, Shen H, Jiang Y, Wang W, Jin J. Novel and low reflective silicon surface fabricated by Ni-assisted electroless etching and coated with atomic layer deposited Al2O3 film. Applied Physics A. 2013;114(3):813-817.

23. Wank J, George S, Weimer A. Nanocoating individual cohesive boron nitride particles in a fluidized bed by ALD. Powder Technology. 2004;142(1):59-69.

24. Digne M, Sautet P, Raybaud P, Euzen P, Toulhoat H. Hydroxyl Groups on γ-Alumina Surfaces: A DFT Study. Journal of Catalysis. 2002;211(1):1-5.

25. Wiedmann M, Jackson D, Pagan-Torres Y, Cho E, Dumesic J, Kuech T. Atomic layer deposition of titanium phosphate on silica nanoparticles. Journal of Vacuum Science & Technology A: Vacuum, Surfaces, and Films. 2012;30(1):01A134.

26. Vannice M. Kinetics of catalytic reactions. 1st ed. New York: Springer; 2005.

27. Oxford University Chemistry Department. Operating Principles - Surface Analysis Facility [Internet]. Saf.chem.ox.ac.uk. 2008 [cited 20 April 2017]. Available from: http://saf.chem.ox.ac.uk/operating-principles-3.aspx

28. Lu N, Khorshidi M. Mechanisms for Soil-Water Retention and Hysteresis at High Suction Range. Journal of Geotechnical and Geoenvironmental Engineering. 2015;141(8):04015032.

29. Green J, Bunshah R. Handbook of Deposition Technologies for Films and Coatings, 2nd Ed. 1st ed. Norwich: Elsevier Science; 1994.

APPENCIX A: EQUATIONS NOTATION

A	specific surface area m^2/g
Ar	Archimedes number
C	BET constant
d	diameter of the reactor (m)
d_g	diameter of the gas molecule (m)
d_p	diameter of the particle (m)
E	reactant exposure (L)
g	acceleration due to gravity (m^2/s)
k	Boltzmann's constant (J/K)
Kn_p	Knudsen number of the particle
λ	mean free path of gas molecules (m)
μ	gas viscosity (Pa·s)
p	pressure of the reactor (Pa)
P	pressure (Pa)
P_o	adsorbate vapor pressure (Pa)
ρ	gas density (kg/m^3)
Re_{mf}	Reynolds number at minimum fluidization conditions
ρ_s	particle density (kg/m^3)
T	absolute temperature (K)
t_p	reactant exposure time (s)
u_{mf}	minimum fluidization velocity (m/s)
V	total volume of gas adsorbed (m^3)
V_m	volume of gas adsorbed at monolayer coverage (m^3)
vp	reactant vapor pressure (Pa)

APPENDIX B: SAMPLE CALCULATIONS

Calculations for Minimum Fluidization Velocity

Units

$mtorr := torr \cdot 10^{-3}$ $\quad pm := 10^{-12}\ m$

Reactor Conditions and Properties

$T := 398\ K$ $\quad p := 91\ mtorr$ $\quad d := 9.5\ mm$

Argon Gas Properties

$mw := 39.948\ \frac{gm}{mol}$ $\quad \mu := 22.62 \cdot 10^{-6}\ Pa \cdot s$ $\quad d_g := 188\ pm$

$$\rho := mw \cdot \frac{p}{T \cdot R} = \left(1.465 \cdot 10^{-4}\right) \frac{kg}{m^3}$$

Gamma-alumina Powder Properties

$d_p := \left(\frac{425 + 180}{2}\right) micron$ $\quad \rho_s := 3.65\ \frac{gm}{cm^3}$

Minimum Fluidization Velocity

$$\lambda := \frac{k \cdot T}{\sqrt{2} \cdot \pi \cdot p \cdot d_g^{\,2}} = 0.288\ cm \qquad Ar := \frac{g \cdot d_p^{\,3} \cdot \rho \cdot (\rho_s - \rho)}{\mu^2} = 0.284$$

$$Kn_p := \frac{\lambda}{d_p} = 9.535$$

$$Re_{mf} := \sqrt{\left(\frac{0.909}{Kn_p + 0.0309}\right)^2 + 0.0357 \cdot Ar} - \left(\frac{0.909}{Kn_p + 0.0309}\right) = 0.043$$

$$u_{mf} := \frac{Re_{mf} \cdot \mu}{\rho \cdot d} = 70.516\ \frac{cm}{s}$$

Volumetric Flow Rate of the Gas

$$Q := u_{mf} \cdot \pi \cdot \frac{d^2}{4} = 49.984\ \frac{cm^3}{s} \qquad \frac{Q}{760} = 3.946\ \frac{cm^3}{min}$$

Calculations for Reactant Exposure Time

Units

$$Langmuir := 10^{-6}\ torr \cdot s$$

Vapor Pressure of Precursors

$$P_{h2o} := 9.2\ torr \qquad P_{TMA} := 4.87\ torr$$

Pulse Times for Target Exposure

$$t_{h2o} := \frac{10^9\ Langmuir}{P_{h2o}} \qquad t_{h2o} = 1.812\ min$$

$$t_{TMA} := \frac{10^9\ Langmuir}{P_{TMA}} \qquad t_{TMA} = 3.422\ min$$

Author's Biography

Born on April 4, 1995, Natalie Altvater grew up in small town Perry, Maine where she was homeschooled until she graduated high school in 2013. She is currently a student at the University of Maine in Orono studying Chemical Engineering, Class of 2017. At the University, she is affiliated with several groups including Engineers Without Borders, American Institute of Chemical Engineers, and Tau Beta Pi. After graduation, she will attend the University of Wisconsin Madison in pursuit of a Ph.D. in Chemical Engineering.